RZ 3486 (# 93952) 03/03/03
Mathematics & Physics 22 pages

Research Report

Tunneling Magnetoresistance and Scanning Tunneling Microscopy with Polarized Electrons

S.F. Alvarado

IBM Research
Zurich Research Laboratory
8803 Rüschlikon
Switzerland

LIMITED DISTRIBUTION NOTICE

This report has been submitted for publication outside of IBM and will probably be copyrighted if accepted for publication. It has been issued as a Research Report for early dissemination of its contents. In view of the transfer of copyright to the outside publisher, its distribution outside of IBM prior to publication should be limited to peer communications and specific requests. After outside publication, requests should be filled only by reprints or legally obtained copies of the article (e.g., payment of royalties). Some reports are available at http://domino.watson.ibm.com/library/Cyberdig.nsf/home.

IBM Research
Almaden · Austin · Beijing · Delhi · Haifa · T.J. Watson · Tokyo · Zurich

Tunneling Magnetoresistance and Scanning Tunneling Microscopy with Polarized Electrons

S.F. Alvarado

IBM Research, Zurich Research Laboratory, 8803 Rüschlikon, Switzerland

Abstract

The controlled injection of spin-polarized charge carriers from a ferromagnetic material into a semiconductor has lately become one of the most important topics in solid-state physics because of the potential advantages of controlling the electron spin in electronic switching devices. Prerequisites for the realization of spintronic devices are (1) The efficient injection of highly polarized electrons at a ferromagnetic-semiconductor interface, and (2) the spin-sensitive detection of the injected electrons. Since the first report in 1975 of spin-dependent transport in a tunnel junction composed of two ferromagnetic layers separated by an insulating barrier, the field of spintronics has made considerable experimental and theoretical progress. A major challenge in the research field of spintronics is the achievement of polarized-electron injection at the junction formed between a ferromagnetic metal (FM) and a semiconducting (SC) material. So far the achieved degree polarization of the electrons injected at a metal/semiconductor junction has been modest. However, tunneling experiments in which electrons are injected through a vacuum barrier from the ferromagnetic metal into a semiconductor show that a spin polarization much higher than hitherto demonstrated should be achievable in a FM/SC junction.

Tunneling Magnetoresistance and Scanning Tunneling Microscopy with Polarized Electrons

S.F. Alvarado
IBM Research
Zurich Research Laboratory
CH - 8803 Rüschlikon, Switzerland

"The magnetic spin valve effect is a modulation of the electrical resistance experienced by spin-polarized electrons flowing between two magnetic materials, occurring when their relative magnetization is switched."

Introduction

The idea to use electronic devices that exploit the electron spin has become a very intensely discussed topic lately, leading to the appearance of the field of "spintronics" [1]. Spin-polarized electron injection into semiconductors is a research topic of growing interest because of the potential advantages offered by the combination of magnetic sensors and storage with electronic readout in a single device. The nature of spintronic devices is expected to allow the fabrication of new magnetically-driven transistors, "spin-transistors," a new generation of memory devices and sensors, and might be of relevance for spin-based quantum information processing. Most spintronic devices proposed so far are based on the spin-valve effect [2]; newly discovered effects, such as magnetization switching by spin-polarized current injection, open up new and exciting possibilities [3]. Finding a means to generate, control, and detect spin-polarized charge carriers represents an important challenge in the realization of spin-based electronics. Furthermore, sources of highly spin-polarized charge carriers are needed, that is, materials having a high degree of spin polarization $P(E_F)$ of the conduction electrons:

$$P(E_\mathrm{F}) = \frac{n_\uparrow - n_\downarrow}{n_\uparrow + n_\downarrow}, \qquad (1)$$

where $n_\uparrow$ ($n_\downarrow$) is the density of spin-up (spin-down) electrons at the Fermi level E_F. From a device point of view, a major breakthrough would be to have devices operating at room temperature.

For this purpose the 3*d* transition ferromagnets Fe, Ni, and Co, and some of their alloys and oxides, are of interest because they have ferromagnetic-to-paramagnetic transition temperatures, T_C, well above room temperature, and exhibit a high degree of spin polarization at the Fermi level. The need for a high T_C is underlined by the fact that the temperature dependences of the bulk and the surface magnetization differ because of the larger spin

fluctuations at the surface region. This is a result of the lack of translational invariance perpendicular to the surface and the reduced number of neighbors of surface atoms compared with bulk atoms. Therefore, the degree of magnetic order of the surface region is significantly lower than that of the bulk. This leads to a roughly linear decrease of the surface magnetization with temperature, in contrast to the curved decrease of the bulk magnetization (see Fig. 1). A criterion for such a surface behavior is that the magnetic coherence length, typically a few lattice constants, is much smaller than the sample thickness. For example for a ferromagnet with $T_C = 600$ K, the surface magnetization is approximately $M_s(T) \approx 0.5\ M_b(0)$ at room temperature, whereas the bulk magnetization $M_b(T) \approx 0.96\ M_b(0)$, where $M_b(0)$ is the saturation magnetization at 0 K. Figure 1 shows, as an example, the surface boundary magnetization of $La_{0.67}Sr_{0.33}MnLaO_3$ measured using spin-sensitive photoelectron spectroscopy (SPES), which has an estimated probing depth of 0.5 nm [4]. Similar results have been obtained for the surface magnetization of Ni by means of spin-polarized, low-energy-electron diffraction [5a], see Fig. 1b, and in Fe_3O_4 [5b].

The band theory of ferromagnets predicts that ferromagnetic materials can be classified into two types: those in which the density of states (DOS) at the Fermi level is predominantly of the majority type, $P(E_F) > 0$, and those where it is of the minority type, $P(E_F) < 0$. Fe [6]

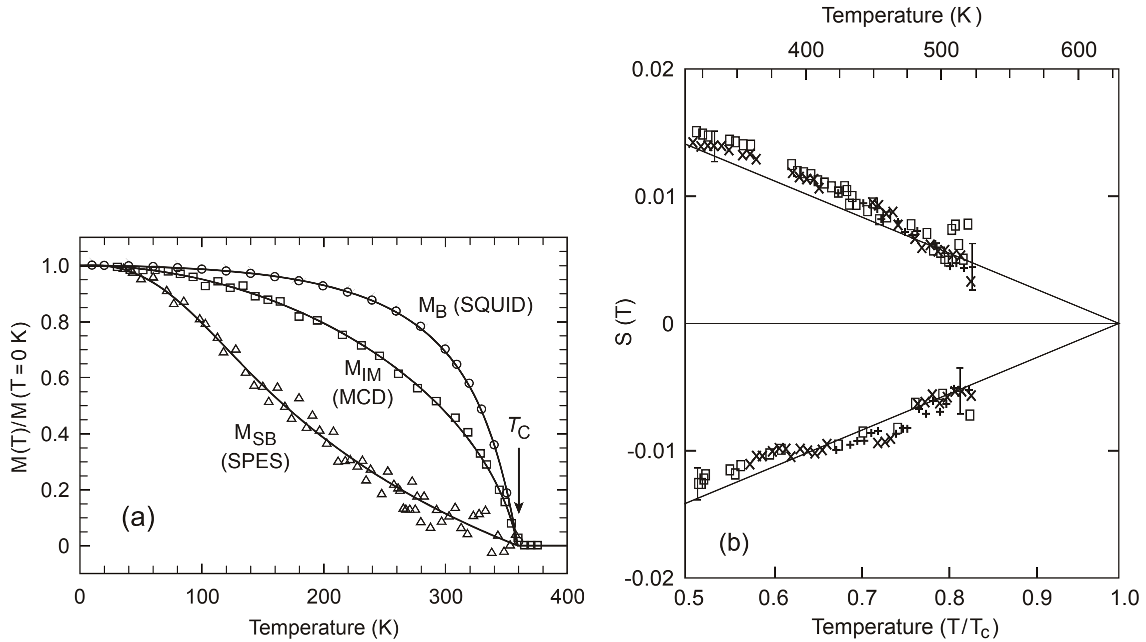

Figure 1. (a) Temperature dependence of the surface boundary magnetization (M_{SB}) of $La_{0.67}Sr_{0.33}MnLaO_3$ measured by SPES at a probing depth of 0.5 nm. For comparison the magnetization of the bulk (M_B) measured by SQUID as well as the magnetization (M_{IM}) measured by soft x-ray magnetic circular dichroism (MCD) at an intermediate probing depth of 5 nm are shown. From Ref. [4]. (b) Temperature dependence of the surface magnetization of Ni(110) measured by means of the scattering asymmetry, S, in spin-polarized low-energy-electron diffraction. From Ref. [5a].

belongs to the first type, whereas Ni [7] and Co [8], where the majority-spin band is completely filled [$n_{\uparrow}(E_F) = 0$], belong to the second class. Figure 2 schematically shows the spin-polarized 3*d* DOS and the spin polarization vs. binding energy, E_B, for Fe and Ni. Magnetic oxides can be classified in a similar manner, for instance, the half-metallic ferromagnets CrO_2 [9] and $La_{0.67}Sr_{0.33}MnLaO_3$ [10] (LSMO) belong to the first class, whereas the half-metallic ferrimagnet Fe_3O_4 (magnetite) belongs to the second class [11,12]. Although in the transition-metal ferromagnets there are *s*- and *p*-electrons at the Fermi level, which are weakly spin polarized, the DOS of the *d*-levels is much greater, making it possible to have a highly polarized total DOS.

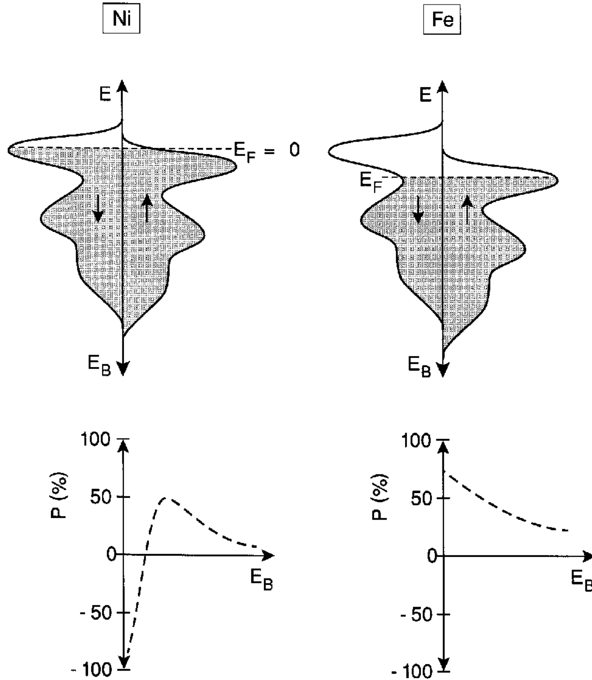

Figure 2. Schematic of the DOS of the 3*d* levels for Fe and Ni. For Fe the spin polarization is positive (dominant majority, ↑-spin) DOS, whereas in Ni the spin polarization is negative (dominant minority, ↓-spin) DOS. The lower panels illustrate the spin polarization vs. binding energy.

That these materials can be sources of highly polarized electrons was demonstrated in 1970 by pioneering photoelectron-emission spectroscopy experiments [13]. The spin polarization of the electron states is obtained from SPES experiments, provided one corrects for the spin-dependent scattering [14] during the transport of the photoexcited electrons to the surface. For instance, SPPES experiments on atomically clean surfaces of Fe [15], Ni [16], and magnetite [12] agree reasonably well with the theoretical predictions. The results on the ferromagnets Fe and Ni show that for some crystallographic directions the photoemitted electrons can exhibit $P(E_F) \approx 90\%$ and $P(E_F) = -95\%$, respectively.

Tunneling of Spin-Polarized Electrons through Barriers Consisting of Insulating Materials: Planar Junctions

In 1971 Tedrow and Meservey [17,18] demonstrated the injection of spin-polarized electrons from a 3*d* ferromagnet (FM) into superconducting aluminum by quantum tunneling across an

insulator (I) Al_2O_3. In these experiments the superconducting films acts as a spin-polarized detector when a magnetic field is applied to the transition-metal FM/I/Al structure. This field defines the orientation of the magnetic moment and therefore the quantization axis for the spin in the magnetic film. It also induces a splitting of the time-reversed states, $k_\uparrow$ and $k_\downarrow$, of the paired quasiparticles in the superconductor, which exhibit an energy gap of 2Δ at the Fermi level and are sharply peaked, into spin-up and spin-down states separated by an energy of $\pm\mu H$, where μ is the electron-spin magnetic moment. The Zeeman splitting of the spin states provides the basis for using a superconductor material in spin-polarized tunneling because at an energy (relative to the Fermi level) of $+\Delta + \mu H$, all electrons in the tunnel current will be of one spin direction, and at $+\Delta - \mu H$ all will be of the opposite direction.

By analyzing the current flowing through the tunnel junction as a function of the applied voltage, the spin-up (majority) and the spin-down (minority) contribution of the current, $I_\uparrow$ and $I_\downarrow$, respectively, injected from energy levels close to the Fermi level of the ferromagnet into the superconductor, can be determined. From this the spin polarization, defined as

$$P = \frac{I_\uparrow - I_\downarrow}{I_\uparrow + I_\downarrow}, \qquad (2)$$

was found to be 44% for Fe, 34 % for Co and 11% for Ni.

For the interpretation of these results it was assumed that at E_F the contributions to the tunneling current, $I_\uparrow$ and $I_\downarrow$, were proportional to the corresponding up- and down-spin DOS, $n_\uparrow$ and $n_\downarrow$, of the ferromagnets. Viewed in this way, these results were surprising because the sign of the spin polarization of Ni and Co was opposite to that predicted by theory and observed in PES experiments. Arguably, the assumption that the tunnel current of each spin channel is proportional to the corresponding DOS is too simplistic, because in a real ferromagnet different states have different effective masses and velocities. Hence it might be more adequate to take a suitably weighted DOS for each electron spin. For instance, Herz and Aoi [19] argued that *s*-electrons are favored over *d*-electrons in tunneling, despite the much greater DOS of *d*-states in the ferromagnets. Calculations of the hopping integrals for the transmission of *s*, *p* and *d*-like electrons across tunneling barriers were carried out, taking into account the electronic structure of the ferromagnets [20-22]. Stearns [23] related the spin polarization of the tunneling current to the relative difference in the momentum, $k_\uparrow(E_F)$ and $k_\downarrow(E_F)$, of the itinerant *d*-like states from the band structure of the ferromagnets. In other theoretical studies the metal is described as a free-electron system, an assumption which is perhaps too simplistic a description of the 3*d* metals [2,24].

In the above-mentioned theoretical analyses an ideal, clean ferromagnetic surface is assumed at the metal–insulator interface. This, however, does not necessarily hold in real planar

junctions, where the metal surfaces are in intimate contact with the insulating material. Chemical bonding at the metal/oxide or metal/semiconductor interface will in most of the cases have a strong impact on the DOS and its spin polarization. This point will be discussed in more detail below.

Tunneling Magnetoresistance: The Invention of the First Spin Valve

An important advance was reported in 1975 by Jullière [25], who replaced the superconducting film of the FM/I/Al tunneling junction by another ferromagnetic metal film. He reasoned that electrons originating from one spin state of the Fermi level of one of the ferromagnetic films would tunnel into unfilled states of the same spin at the Fermi level of the other ferromagnetic film. Provided that the up- and down-spin DOS at the Fermi level of each ferromagnet are different, it is easy to see that the electric resistance of the tunnel junction is expected to change by reversing the relative magnetization of the ferromagnetic layers from parallel (R_P) to antiparallel (R_{AP}). This is in fact what he observed in a tunnel junction consisting of Co/Ge/Fe, where a change in the conductance of $\Delta G/G_P$ = 14% was seen at 4.2 K [25]. Maekawa and Gäfvert [26] found a change of a few percent in the magnetoresistance in magnetic tunnel junctions at 4.2 K with NiO as barrier material. The magnetic spin valve demonstrated by Jullière straightforwardly exploits the spin-dependent DOS at the Fermi level of the two ferromagnets to influence spin-polarized charge-carrier transport. Figure 3 illustrates the principle of devices of this type.

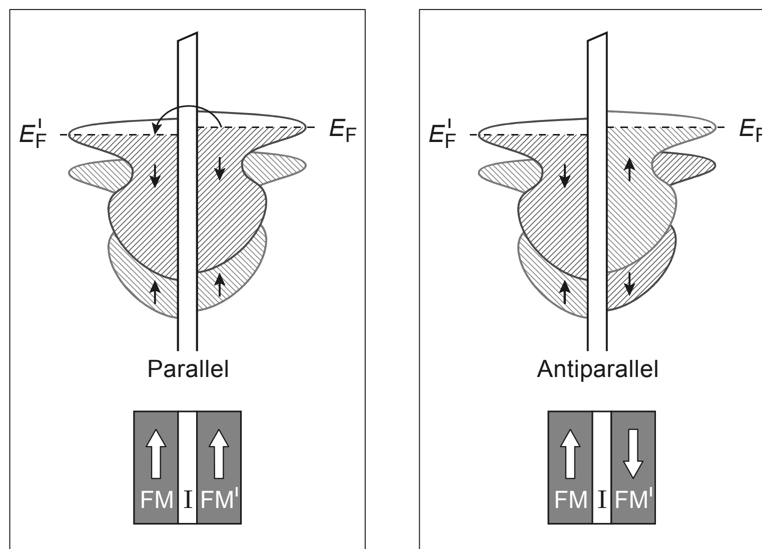

Figure 3. Schematic of a TMR device consisting of two ferromagnetic thin films, FM and FM', separated by a tunneling barrier made of an insulating material, I. The current flow for parallel and antiparallel alignment of the magnetic moments of the ferromagnetic film is shown.

In 1995, large room-temperature values of the tunneling magnetoresistance (TMR) ratio $\Delta R/R_\mathrm{P} \approx 22\%$ [27] and 15% [28] were reported. This discovery triggered intense research activities towards understanding the injection, transport, and detection of spin-polarized current in order to optimize spin-valve devices. Recently tunnel junctions exhibiting room- temperature magnetoresistance ratios close to 40% have been demonstrated [29]. These tunneling devices are promising for applications such as magnetic random-access memories (MRAM) [29], and some applications are already under development.

The Jullière Model

The model most widely used today to describe the magnetotransport of tunnel junctions is that of Jullière [25], which was inspired by the ideas of Tedrow and Meservey [17,18]. The basic idea is that for the ferromagnet FM (FM') the tunneling current consists of a fraction of electrons $N_\uparrow$ ($N'_\uparrow$) whose magnetic moments are parallel to the magnetization, i.e., majority electrons, and a fraction of electrons with antiparallel orientation, i.e., minority electrons, is $N_\downarrow$ ($N'_\downarrow$). Hence, the conductance of the tunnel junction, at $V = 0$, is proportional to

$$G_\mathrm{P} = N_\uparrow N'_\uparrow + N_\downarrow N'_\downarrow \tag{3}$$

for parallel magnetization and to

$$G_\mathrm{AP} = N_\uparrow N'_\downarrow + N_\downarrow N'_\uparrow \tag{4}$$

for antiparallel magnetization of the ferromagnetic films.

Assuming spin conservation during transport, the relative conductance variation is given by

$$\frac{\Delta G}{G} \equiv \frac{G_\mathrm{P} - G_\mathrm{AP}}{G_\mathrm{P}} = \frac{2PP'}{1+PP'}, \tag{5}$$

where $P = (N_\uparrow - N_\downarrow)/(N_\uparrow + N_\downarrow)$.

From Eq. (5), the TMR is

$$\mathrm{TMR} = \frac{\Delta R}{R_\mathrm{AP}} \equiv \frac{R_\mathrm{AP} - R_\mathrm{P}}{R_\mathrm{AP}} = \frac{2PP'}{1+PP'}. \tag{6}$$

The TMR is said to be “normal” if it is positive, i.e. $R_\mathrm{AP} > R_\mathrm{P}$, and “inverse” if it is negative, i.e., $R_\mathrm{AP} < R_\mathrm{P}$.

Note: Some authors prefer to use the “optimistic” definition:

$$\frac{\Delta R}{R_\mathrm{P}} = \frac{R_\mathrm{AP} - R_\mathrm{P}}{R_\mathrm{P}} = \frac{2PP'}{1-PP'}, \tag{7}$$

while others use

$$\frac{\Delta R}{R} = \frac{R_{\mathrm{AP}} - R_{\mathrm{P}}}{R_{\mathrm{P}} + R_{\mathrm{AP}}} = 2PP'. \quad (8)$$

Jullière's model is very useful for practical purposes, but for an in-depth interpretation of experimental data one has to be aware of limitations arising from several important assumptions made. In the original model, it is assumed that P and P' are the spin polarizations of the Fermi-energy DOS of the two ferromagnetic metals. This interpretation is based on the conventional theory of tunneling, where the tunneling current is proportional to the product of the unperturbed DOS [Eqs. (3) and (4)]. Other important assumptions implicit in the model are that the TMR depends neither on the geometry of the barrier (height and thickness) nor on its electronic structure, and that the direction of the electron spin is conserved during transport.

Influence of the Interface on the Spin Polarization of Tunneling Electrons

In a real FM/I/FM, the spin polarization of the charge carriers is not necessarily a fundamental property of the bulk ferromagnet, but rather is related to the electronic structure and transport properties of the particular ferromagnet/insulator interface as well as the electronic structure of the material the tunneling barrier consists of. The spin polarization depends on the character of the electronic states at the ferromagnet/insulator interface. Bonding effects at the interface, for instance, can modify the electronic states at the surface of the ferromagnet. This has been shown by experiments on magnetic junctions made with various barrier materials. Thus, in tunnel junction of the type FM/I/LSMO, it is found that using a Co electrode, $P > 0$ for an Al_2O_3 barrier, whereas $P < 0$ for $SrTiO_3$ and $Ce_{0.69}La_{0.31}O_{1.845}$ barriers [30]. This is consistent with theoretical studies [31-34] showing that the spin polarization of the tunneling electrons is governed by the specific type of electronic bonding at the interface. In particular, self-consistent band-structure calculations [32] of the Co/Al_2O_3 interface account for the observed positive polarization in terms of the strong bonding between the minority-spin *d*-orbitals of Co and the *sp* orbitals of the Al at the interface and the resulting reduction of the minority-DOS in Co.

Injection of Spin-Polarized Electrons into Semiconductors

> "We stand today on the verge of a 'magnetoelectronics' revolution in which these new phenomena will be not only explained but also exploited, in devices combining magnetism with traditional electronic elements."
> G. Prinz and K. Hathaway, Ref. [1]

Beyond multilayered TMRs of the type described above, other device architectures can be imagined. A field-effect transistor (FET) that works as a spin valve was proposed by Datta and Das [35]. This is a three-terminal structure in which the spin-polarized carriers of a two-dimensional electron gas (2DEG) confined in a semiconducting material are injected by a

ferromagnetic source and then detected by a ferromagnetic drain. The initial direction of the polarization is defined by the magnetization of the injecting contact, whereas the extracting contact functions as a spin analyzer. As the electrons traverse the 2DEG, the spin vector is controlled via the precession caused by the spin-orbit interaction, which is varied by an external electric field perpendicular to the 2DEG. The function of the gate is to control this field, and, accordingly, via the orientation of the electron spin, the current at the extracting contact. In such a device, resistance modulation can also be achieved by having ferromagnetic contacts with different magnetic coercitivities, permitting parallel or antiparallel magnetization orientation to be established at will by means of an applied magnetic field [36].

Prerequisites for the realization of efficient spintronic devices are (i) efficient injection of spin-polarized charge carriers from a magnetic material into a semiconductor, (ii) a long spin-relaxation time, τ_s, and (iii) an efficient detection of spin-polarized charge carriers flowing from a semiconductor into a magnetic material. Regarding requirement (ii), it is known that GaAs, for instance, exhibits τ_s in the range of 0.1 to 1 ns, corresponding to spin-diffusion lengths of $l_s \approx 1$ μm at room temperature and of several micrometers at 10 K [37]. Spin-relaxation times as long as 0.1 μs ($l_s \approx 100$ μm) were observed at 5 K on *n*-doped GaAs [38]. Note that τ_s depends on the doping type and concentration, crystal quality, etc. Regarding the injection of polarized electrons, two kinds of sources of spin-polarized electrons have been tried, namely, magnetic semiconductors and ferromagnetic metals.

Ohno *et al*. [39], using the ferromagnetic semiconductor $Ga_xM_{1-x}As$ as a spin aligner, demonstrated spin-polarized electron injection into GaAs leading to a relative change of the degree of circular polarization of the electroluminescence of more than 1%. A degree of spin polarization of the injected current of 90% was obtained by Fiederling *et al*. [40] at 4 K by using paramagnetic $Be_xMn_yZn_{1-x-y}Se$ to align the electron-spin orientation. For potential spintronic applications, however, both of these sources of spin-polarized electrons have the huge drawback of being restricted to very low temperatures because they are either paramagnetic or exhibit Curie temperatures in the range of 10 to 100 K. Obvious candidates for room-temperature applications are ferromagnetic metals such as Fe, Ni, Co, their alloys, and oxides having a high T_C. The reactivity of the transition metals with most semiconductors (SC), however, can give rise to magnetically "dead" layers at the interface of the FM/SC contact, hampering efficient spin injection into the semiconductor. In addition, fundamental problems seem to limit the spin polarization of electrons injected even in the case of an ideal, unreacted, interface. Theoretical studies show that in electrical spin injection from a ferromagnetic metal into a semiconductor interface, the polarization of the charge carriers becomes very small when its conductivity, σ_{fm}, is much higher than that of the semiconductor, σ_{sc}. Thus by solving the spin-transport equations at a magnetic/nonmagnetic inter-

face, van Son *et al.* [41] calculate the spin polarization of the current injected into the nonmagnetic material. If the latter is a semiconductor, the results reads

$$P_j = P\frac{\sigma_{\rm sc}}{\sigma_{\rm fm}}\frac{\lambda_{\rm fm}}{\lambda_{\rm sc}}\frac{2}{1-P^2}. \tag{9}$$

This result should be valid if

$$\frac{\sigma_{\rm fm}}{\sigma_{\rm sc}}\frac{\lambda_{\rm sc}}{\lambda_{\rm fm}} >> (1-P^2)^{-1}, \tag{10}$$

where $\lambda_{\rm fm}$, $\lambda_{\rm sc}$ are the spin-diffusion lengths and P is the spin polarization of the charge carriers in the metal.

By definition the spin-injection efficiency is $\eta = P_i / P$.

For a semiconductor at room temperature $\lambda_{\rm sc}$ can be of the order of a few micrometers, whereas $\lambda_{\rm fm}$ is of the order of several nanometers, and $\sigma_{\rm fm} \sim 10^4 \sigma_{\rm sc}$, from which one obtains that $P_j << 1\%$. Schmidt et al. [42] reported on calculations of electrical spin injection into a semiconductor structure, which is contacted by two ferromagnetic metals separated by a distance x_0 from each other, such that $x_0 << \lambda_{\rm sc}$. The main insight of that study is that the basic obstacle for spin injection from a ferromagnetic metal into a semiconductor originates from the large conductivity mismatch between the two materials. Thus, given condition (10), in which $\lambda_{\rm sc}$ is replaced by x_0, the polarization of the injected charge carriers is

$$P_j = p\frac{\sigma_{\rm sc}}{\sigma_{\rm fm}}\frac{\lambda_{\rm fm}}{x_0}\frac{2}{1-P^2}. \tag{11}$$

Hence for a spin-injection device with $x_0 \approx 1\,\mu$m, one finds that $P_j << 1\%$. Furthermore, the difference in resistance between the parallel and antiparallel magnetization configurations is $\Delta R / R \approx P_j^2$ [42].

Note, however, that in those calculations a "perfect" ohmic contact is assumed. In reality, however, the situation can be very different because a Schottky barrier is typically formed at a metal/semiconductor interface. In fact theoretical studies indicate that either a Schottky [43,44] or a tunneling barrier[45-47] can be a way to circumvent the limitations posed by the conductivity mismatch. A theoretical study shows, in addition, that electric field effects can enhance the spin injection efficiency by several orders of magnitude [48].

The first experimental demonstration of electrical spin injection from a ferromagnetic metal into a semiconductor was reported in the early 1990s [49-51]. In these scanning tunneling microscope-based (STM) experiments, a spin polarization of up to 35% at room temperature, was achieved for electrons injected from ferromagnetic metal tips trough a tunneling barrier

into III-V compounds. These experiments, which shall be discussed in more detail below, are proof that the limitations imposed by the conductivity mismatch and/or by chemical reactions between the ferromagnet and the semiconductor at the interface can be circumvented by intercalating a tunneling barrier. Note that the spin-polarized electron-injection experiment using the STM has been recently performed at 100 K using Ni tips and GaAs [52,53]. Regarding FM/SC contact junctions, however, the realization of efficient electrical injection of highly spin-polarized electrons has so far proven to be a great challenge. For instance, experiments performed on spin-valve devices based on semiconductors with lateral metal electrodes showed efficiencies below 1% [54-56]. Hammar *et al.* [57] report on spin injection from a ferromagnet into the spin-split states of a 2DEG, where interface-resistance changes of about 1% at room temperature are interpreted as being due to an interfacial current polarization of 20%. These results are, however, the topic of debate [58]. Recently a 2% polarization of injected electrons was achieved for light-emitting diodes (LED) consisting of a Fe thin films grown on a GaAs/InGaAs structure [59], and a value of at least 4% has been reported for a Fe film grown on a GaAs/AlGaAs structure [60] at room temperature. In these latter experiments the polarization of the injected charge carriers is determined by measuring the degree of circular polarization of the emitted light. Recently LEDs using metal/insulator/semiconductor structures, where the insulator Al_2O_3 acts a tunnel barrier, have been demonstrated. So far the polarization of the injected charge carriers is about 1% at room temperature [61] and 9% at 80 K [62].

Injection of Spin-Polarized Electrons into Semiconductors through a Vacuum Barrier

In contrast to the low degree of polarization for electrons injected across Fe/GaAs contacts, a spin polarization that is one order of magnitude higher has been achieved at room temperature by electron tunneling from ferromagnetic Ni across a vacuum barrier into the conduction band of atomically clean *p*-doped GaAs surfaces [49,51]. These experiments have been carried out with an STM, in which a ferromagnetic metal tip is used as a source of spin-polarized electrons. Figure 4 shows a schematic of the experimental arrangement, and Fig. 5 shows a schematic of the energy diagram of the tunneling junction. The spin polarization of the electrons injected into the semiconductor is determined by measuring the circular polarization of the recombination luminescence. The spin-detection scheme is explained in Fig. 6. For a more detailed description of the relation between the spin polarization of conduction electrons and photon absorption/emission in III-V compounds, see the Course Notes of M. Dyakonov in this book. Injection across a tunneling barrier has the advantage that interface effects, such as chemical bonding between the ferromagnetic material and the semiconductor, can practically be eliminated. This is demonstrated by the results obtained on Ni and Fe, which reveal that the polarization of electrons emitted from an energy range close to the Fermi level is negative (minority polarization) for Ni and positive (majority) for Fe [50].

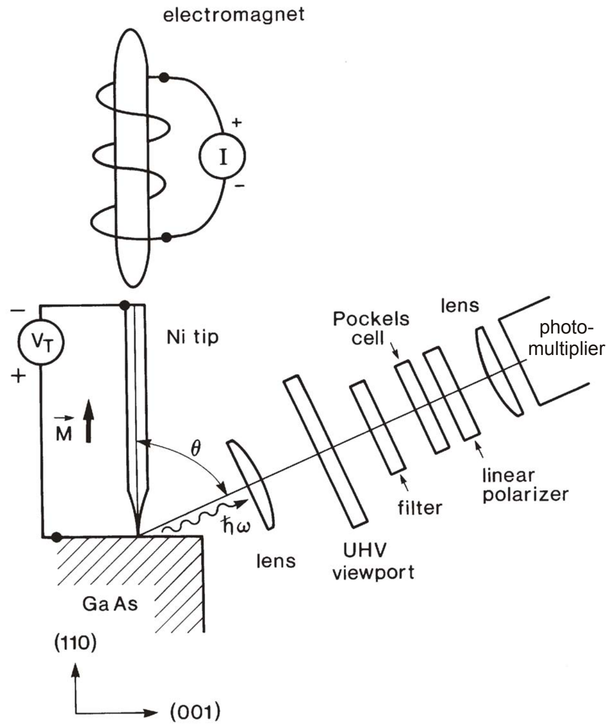

Figure 4. Experimental arrangement used for tunneling injection of highly polarized electrons from a ferromagnet into the conduction band of a semiconductor. The spin-polarized electron injection efficiency is detected by measuring the helicity of the radiation emitted upon recombination of the injected charge carriers.

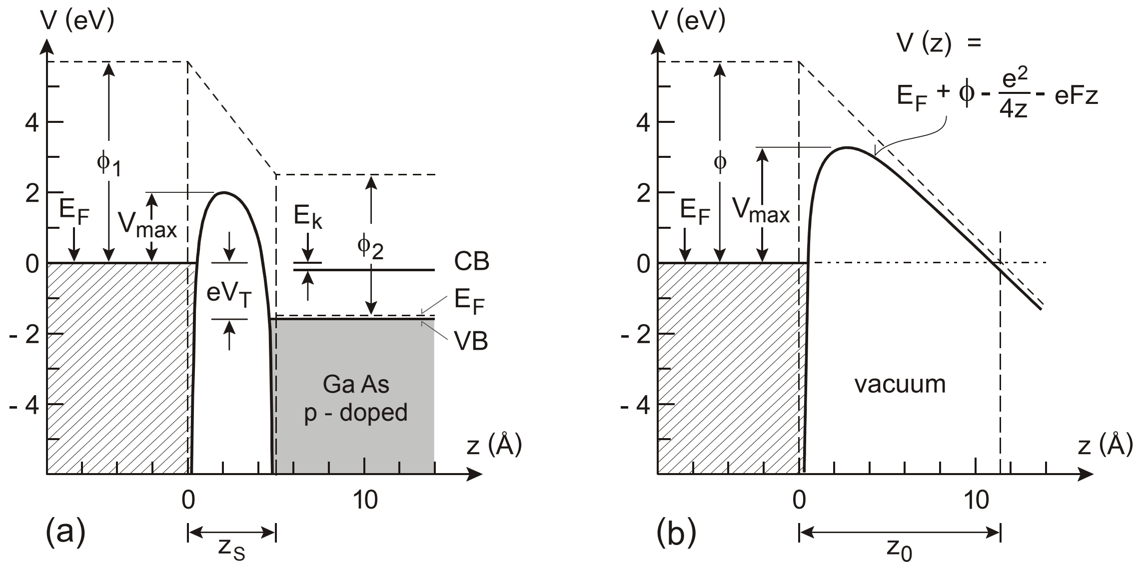

Figure 5. (a) Energy diagram for the injection of polarized electrons into a semiconductor across a vacuum tunneling barrier. For a tunneling bias V_T, electrons from the ferromagnetic metal having a binding energy in the range $E_F - E_k < E_B \leq E_F$ are injected into the conduction band (CB) of the semiconductor. $E_k \approx eV_T - E_G$, where E_G is the forbidden band gap. VB is the valence band. (b) Comparative energy diagram for tunneling through a vacuum barrier for the case of field emission.

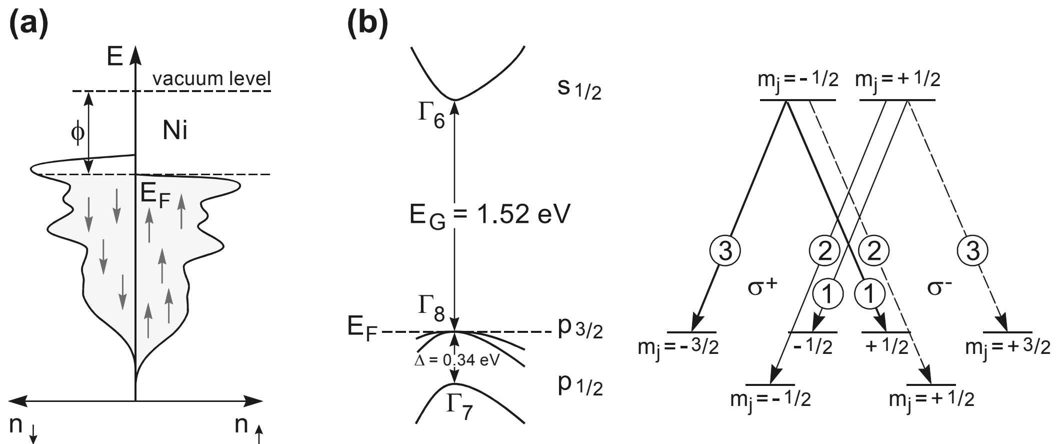

Figure 6. Simplified description of the detection of the spin polarization of electrons injected into the conduction band via measuring the degree of helicity of radiative recombination: Because of the spin selection rule, 100% polarized electrons in the conduction band, e.g., $m_j = -1/2$, recombine into $m_j = -3/2$ and $m_j = +1/2$ states at the (Γ_8) point, giving rise to right- (σ^+) and left-circularly polarized (σ^-) radiation with a relative probability of 3 and 1 (encircled numbers), respectively. Recombination into the split-off (Γ_7) point is suppressed by lack of empty states owing to the relatively large distance from E_F, determined by the spin-orbit coupling Δ. Fully polarized electron recombination thus gives rise to a maximum circular polarization of ρ_L = 50% of the emitted radiation.

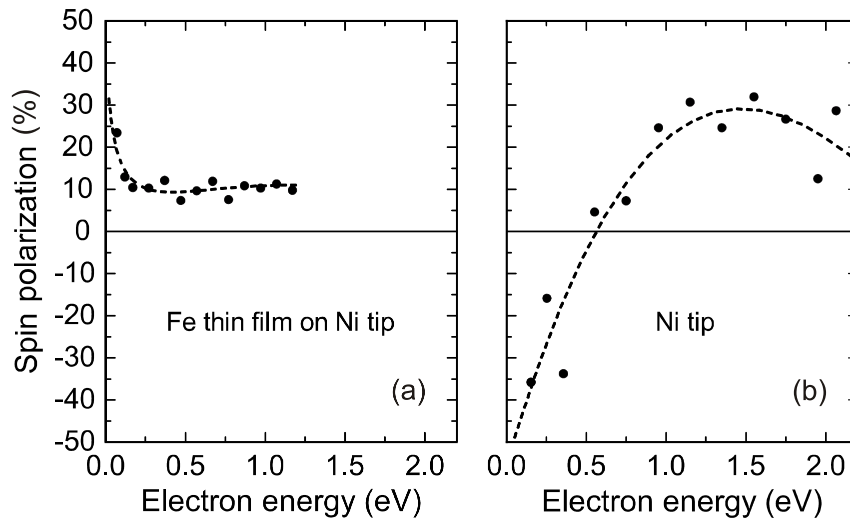

Figure 7. Spin polarization of electrons *vs*. injection energy into GaAs by tunneling through a vacuum barrier from ferromagnetic Fe (a) and Ni (b). Adapted from Ref. [50].

The polarization of electrons injected from Fe and Ni into an AlGaAs alloy as a function of the maximum kinetic energy of the tunneling electrons, E_k, is shown in Fig. 7 [50], see [63]. These results are in qualitative agreement with the spin-polarized DOS of the clean ferromagnetic surface of Fe [13,64,65] and Ni [14,66-71], shown schematically in Fig. 2. Moreover, the fact that chemical bonding effects are practically eliminated in vacuum-tunneling experiments allows new insights into the injection of spin-polarized electrons. For instance, by using the STM it becomes possible to characterize some features of the potential barrier that influence the injection of spin-polarized electrons from a ferromagnetic metal into a metal or a semiconductor.

Dependence of the Electron Spin Polarization on the Details of the Tunneling Potential Barrier

The spin polarization of electrons tunneling from 3*d* ferromagnets through a vacuum potential barrier was first studied by means of spin-polarized field-emission spectroscopy (SPFES) using ferromagnetic metal tips. In these experiments the sign of the spin polarization was found to be positive for Fe [72] and negative for Ni [73-74], as expected from the spin-polarized DOS at E_F, with the exception of Ni(110)-oriented tips for which a positive polarization was found [74]. Surprisingly, in all cases the magnitude of the polarization is below 10%, i.e., much lower than the expected spin polarization of the 3*d* levels at E_F.

In tunneling through vacuum barriers, the electrons emitted from the ferromagnetic metal originate from the highly polarized, localized *d*-like states as well as from the low-polarized, delocalized 4*sp*-like states [75-78]. Maximum spin polarization is generally expected when only the 3*d*-like levels contribute to the tunneling current. Given their highly delocalized nature, however, the *sp*-like states contribute substantially to the tunneling current, despite the fact that their DOS is roughly one order of magnitude smaller than that of the 3*d* levels. Theoretical estimates of the tunneling probability ratio between the 3*d* and the 4*sp* band, $T_d(s)/T_{sp}$, lie in the range of 10^{-2} to 10^{-1} [75-78]. Thus the low degree of polarization found in SPFES is explained by the—relative to the 3*d*—dominant 4*sp* contribution to the tunneling current.

The discrepancy in polarization magnitude found in the SPFES and the spin-polarized STM experiments points to the influence of the differences in the tunneling barriers that are characteristic of the particular experiments. In SPFES, the effect of the barrier geometry on the polarization of tunneling electrons can be studied by varying the thickness and height of the barrier by means of the electric field. In this case, however, the energy range of the tunneling electrons would not remain constant when the field is varied. On the other hand, in STM the geometry of the tunneling barrier can be manipulated by varying the tunneling current while keeping the bias voltage constant. This has the advantage that the energy range from which electrons tunnel is kept constant. Figure 8 shows the spin polarization of

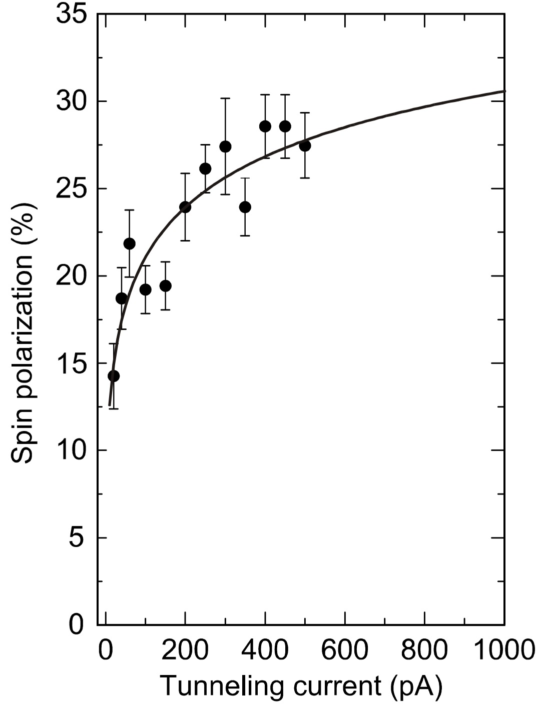

Figure 8. Electron spin polarization *vs*. tunneling current for injection into $Al_{0.06}Ga_{0.94}As$. A ferro–magnetic Ni tip is the source of polarized electrons. Increasing the tunneling current from 20 to 500 pA results in a decrease of the tunneling-barrier thickness by approx. 0.18 nm. The solid line is the result of an analysis of the data, Eq. (17), in terms of a model in which the tunnel current arises from a linear superposition of 3*d*-like and one 4*sp*-like contribution. From Ref. [49].

electrons injected from a polycrystalline Ni tip into an $Al_{0.06}Ga_{0.94}As(110)$ surface [49], see [63]. The tunneling current was varied in the range 20 pA $\leq i_{\mathrm{T}} \leq$ 500 pA, which causes the barrier width (determined by the tip–surface distance) to change by about 0.18 nm. The tunneling bias is V_{T} = 1.8 V, and the binding-energy range probed in the Ni tip is $E_k \leq E < E_{\mathrm{F}}$, where $E_k \approx eV_{\mathrm{T}} - E_{\mathrm{G}} = 300\,\mathrm{meV}$ and E_{G} is the SC band gap. The results show that increasing the tunneling current by a factor of 25 translates into an increase of the spin polarization by about a factor of two, i.e., from –14.3% to –28.6% at room temperature. Note that the spin splitting of the conduction band, induced by the electric field of the host crystal, gives rise to a small residual polarization [79-83]. This effect can be minimized by properly orienting the GaAs(110) surface such that the $[\bar{1},1,1]$ axis is oriented in a direction perpendicular to the optical detection axis [51].

To rationalize how the geometry of the tunneling barrier influences the injection efficiency of spin-polarized electrons, a simple model is proposed that assumes that the total tunneling current, i_{T}, is given by

$$i_{\mathrm{T}} = i_d + i_{sp}\,, \tag{12}$$

where i_d and i_{sp} represent the contributions originating from 3*d*-like states and a 4*sp*-like state. The current for small tunneling energies depends exponentially on the product of the tunneling barrier width, *s*, and the square root of the mean barrier height, $\sqrt{\phi}$, hence

$$i_{\mathrm{T}} = i_{d,0}\exp(-sA\sqrt{\phi_d}) + i_{sp,0}\exp(-sA\sqrt{\phi_{sp}})\,, \tag{13}$$

where $i_{d,0}$ and $i_{sp,0}$ are constants. The decay length κ_j^{-1} for j = *sp*, *d* is related to the mean barrier height by $\kappa = A\sqrt{\phi_j}$, where $A = 2\sqrt{2m}\,\hbar$. Note that the decay length reflects the fact that in the barrier the radial parts of the different wavefunctions decay at different rates. Note also that, because of image forces, ϕ_d is also a function of *s* [84,85].

The polarization *P* of the tunneling electrons is given by

$$i_{\mathrm{T}}P = i_d P_d + i_{sp} P_{sp}\,, \tag{14}$$

where P_d and P_{sp} are the polarization of the 3*d*- and 4*sp*-like states. Assuming $|i_d P_d| >> |i_{sp} P_{sp}|$ [76,78], Eqs. (13) and (14) lead to

$$P(s) = \frac{P_d}{1 + (i_{sp,0}/i_{d,0})\exp\left[sA\left(\sqrt{\phi_d} - \sqrt{\phi_{sp}}\right)\right]}\,, \tag{15}$$

where the coefficient $i_{j,0}$ is proportional to the local DOS near E_{F} multiplied by the non-exponential prefactor of the tunneling matrix element. The quotient of the pertinent prefactors is of the order of unity [86]. Thus one would expect $i_{sp,0}/i_{d,0} \approx 3\times10^{-2}$, which is approximately the ratio of the 4*sp*- to the 3*d*-band densities of states at the Fermi level [87]. Assuming that the relative tunneling probability $T_j \propto i_j$, one obtains $T_{sp}/T_d = i_{sp}/i_d$, and thus Eq. (15) can be rewritten as

$$P(s) = \frac{P_d}{1 + [T_{sp}(s)/T_d(s)]}\,. \tag{16}$$

Equation (15) shows that the characteristic decay length of the electron-spin polarization of the tunneling electrons is a measure of the difference between the mean potential barrier heights, $A\left(\sqrt{\phi_d} - \sqrt{\phi_{sp}}\right)$. Because of their higher degree of spatial localization, the 3*d*-like levels are expected to exhibit a shorter decay length at the surface than the *sp*-like levels [88], implying that $\phi_{sp} < \phi_d$. Hence, with decreasing barrier width, the ratio $T_{sp}(s)/T_d(s)$ increases, favoring the injection of highly polarized electrons by tunneling into the semiconductor.

To quantify the relationship between the degree of spin polarization and the tunneling current in the experimental data for tunneling from a Ni tip into $Al_{0.06}Ga_{0.94}As$, Fig. 8, the following equation can be written, as suggested by the form of Eq. (15):

$$P(s) = \frac{P_d}{1 + Bi_{\mathrm{T}}^{-\gamma}}\,, \tag{17}$$

where P_d and γ are fitting parameters. As the total tunneling current can be expressed approximately by $i_{\mathrm{T}} = i_0 \exp(-sA\sqrt{\phi})$, where $\phi_{sp} < \phi < \phi_d$, we see by comparison with Eq. (15) that γ is simply the ratio between the exponential decay length of the tunneling current and the spin polarization: $\gamma = \left(\sqrt{\phi_d} - \sqrt{\phi_{sp}}\right)/\sqrt{\phi}$. The solid line in Fig. 8 is Eq. (17) fitted to the data. A reasonably good fit of the data can be obtained with values of P_d, which represents the maximum polarization obtainable, in the range of approx. 40% to 90%. The lower value of P_d appears to be the most plausible, considering that, owing to reduced magnetization of the surface region of the ferromagnet (see [4-6], the maximum polarization at the Fermi level is expected to be approx. 50% (in the bulk region it is close to 95%). From this one can estimate that the spin injection efficiency is in the range of 40% to 80% for injection through a vacuum tunneling barrier.

From several measurements, one obtains γ in the range of +0.43 to +0.25. For the results shown in Fig. 8 one can estimate that the probability ratio T_d / T_{sp} increases by more than a factor of two when the current changes from 20 to 500 pA, whereas the barrier width decreases by $\Delta s \approx -0.18$ nm. This is an indication that the 3*d* contribution to the tunneling current can become dominant. The above analysis is done assuming that the polarization of the *sp* states is negligible. An analysis of the data assuming $P_{sp} > 0$ shows that the fitting parameter $i_{sp,0} / i_{d,0}$ *decreases*, roughly by a factor of two, when increasing P_{sp} from 0 to 25%, whereas γ is reduced slightly.

With the aid of Eq. (15) and the fit parameters obtained from the STM data, it is possible to account for the magnitude of the polarization observed in SPFES experiments $(1 \le P \le 10\%)$ by taking a barrier width in the range $0.9 \le s \le 1.3$ nm. This is precisely the thickness range of the tunneling barrier under typical SPFES working conditions [72-74]. Thus the present interpretation of the STM data can also account for the magnitude of the spin polarization measured on Ni tips with FES, and shows that generally a higher tunneling-electron spin polarization can be achieved with STM than with SPFES. Note, however, that in STM and SPFES the energy ranges of the tunneling electrons differ somewhat. Thus in STM the energy distribution has a full width at half maximum (FWHM) in the range of 150 meV or less for the experiments shown in Fig. 8, whereas in FES typically FWHM = 0.2–0.5 eV. This can be of importance in the case of Ni because the highest polarization of the 3*d* levels appears in a narrow energy range, approx. 100 meV below the Fermi level. Note also that the shape of the potential barrier is somewhat different, as illustrated in Fig. 5.

Another technique involving the transfer of polarized electrons through a vacuum barrier is electron-capture spectroscopy (ECS) [89]. Here the basic process is the capture of one or two

spin-polarized electrons during small-angle reflection of 150-keV deuterons at single-crystalline surfaces of ferromagnetic crystals. This is similar to a tunneling experiment because it probes the exponential tail of the electronic states of the surface. For Ni, Fe, and Co, spin-sensitive ECS shows that the polarization strongly depends on the various (*hkl*) orientations of the surfaces. But, most importantly, the magnitude of the spin polarization is very high, for instance –44% to –96% for Ni surfaces. This is not unexpected because in ECS the effective thickness of the tunneling barrier is approximately 0.2 nm [89], and, hence, according to the simple two-channel model described above, the 3*d*-state contributions to the tunneling current largely become dominant, giving rise to highly polarized electron transport from the ferromagnetic surface of the 3*d* metal to the deuterium atoms.

Certainly more sophisticated models and further theoretical work are necessary for a better understanding of the experimental data. For instance, in a recent theoretical study the transmission of *sp*- and *d*-states across vacuum barriers of various thicknesses has been calculated. The equivalent device modeled is an ideal TMR junction with two Co electrodes. The calculations predict a negative spin polarization of decreasing magnitude with barrier thickness for very thin barriers, where *d*-state contributions dominate over *sp* contributions. For thicker barriers, where positively polarized *sp* electron contributions begin to dominate, however, the polarization changes sign with increasing barrier thickness [90].

Summary and Outlook

Current electronics and optoelectronics are based on the transport and storage of electronic charge in semiconductors. Taking advantage of the spin of the charge carriers could revolutionize electronics, leading to novel devices combining magnetism with traditional electronic elements in which electric currents and radiative recombination processes are manipulated by controlling the direction of the electron spin. The foundation of this progress rests in several areas of solid-state physics research:

1. Spin-polarized electronic structure of ferromagnets, particularly at interfaces between different materials.
2. Transport of spin-polarized charge carriers in magnetic materials, semiconductors, insulators, and at their interfaces. This includes tunneling of charge carriers between solids and the influence of the electronic structure of the barrier.
3. Spin-dependent scattering, motion, and control of the spin of charge carriers in transport through ferromagnets and semiconductors.

Acknowledgments

It is a pleasure to thank B. K. Crone, U. Dürig, H. P. Meier, H. W. M. Salemink, G. Salis, and Ch. Schönenberger for help and for fruitful discussions. Many thanks also to R. Allenspach for many useful comments and a critical reading of the manuscript.

References

1. Special Issue on Magnetoelectronics, *Physics Today* 48(4), G. Prinz and K. Hathaway, p. 24 (1995).
2. "Conductance and exchange coupling of two ferromagnets separated by a tunneling barrier," J. Slonczewski, *Phys. Rev. B* 39, 6995 (1989)
3. "Current-driven magnetization reversal and spin-wave excitations in Co/Cu/Co pillars," J. A. Katine, F. J. Albert, and R. A. Buhrman, E. B. Myers, and D. C. Ralph, *Phys. Rev. Lett.* 84, 3149 (2000)
   "Spin-polarized current switching of a Co thin film nanomagnet," F. J. Albert, J. A. Katine, R. A. Buhrman, and D. C. Ralph, *Appl. Phys. Lett.* 77, 3809 (2000)
4. "Magnetic properties at surface boundary of a half-metallic ferromagnet $La_{0.7}Sr_{0.3}MnO_3$," J.-H. Park, E. Vescovo, H.-J. Kim, C. Kwon, R. Ramesh, and T. Venkatesan, Phys*. Rev. Lett.* 81, 1953 (1998)
5. (a) "Surface magnetization of ferromagnetic Ni(100): A polarized low-energy electron diffraction experiment," R. J. Celotta *et al*., *Phys. Rev. Lett.* 43, 728 (1979);
   (b) "Magnetism of surfaces by spin polarized photoemission," S. F. Alvarado, *Z. Phys. B* 33, 51 (1979);
   (c) "Surface magnetism in magnetite single crystals by spin-polarized photoemission," S. F. Alvarado and W. Eib, *J. Magn. Magn. Materials* 7, 16 (1978)
6. "Energy bands in ferromagnetic iron," J. Callaway and C. S. Wang, *Phys. Rev. B* 16, 2095 (1977)
7. "Calculation of spin-polarized threshold photoemission from the Ni(001), Ni(111), and Ni(110) surfaces," R. Clauberg, *Phys. Rev. B* 27, 4644 (1983)
8. *Calculated Electronic Properties of Metals*, V. L. Maruzzi, J. F. Fanak, and A. R. Williams (Pergamon, New York, 1978)
9. "New class of materials: Half-metallic ferromagnets," R. A. de Groot, F. M. Mueller, P. G. van Engen, and K. H. J. Buschow, *Phys. Rev. Lett*. 50, 2024 (1983);
   "CrO_2 - A new half metallic ferromagnet?" K. P. Kämper, W. Schmidt, G. Güntherodt, R. J. Gambino, and R. Ruf, *Phys. Rev. Lett.* 59, 2788 (1988);
   "CrO_2: A self-doped double exchange ferromagnet," M. A. Korotin, V. I. Anisimov, D. I. Khomskii, and G. A. Sawatsky, *Phys. Rev. Lett.* 80, 4305 (1998)
10. "Large magnetotunneling effect at low magnetic fields in micrometer-scale epitaxial $La_{0.67}Sr_{0.33}MnO_3$ tunnel junctions," Y. Lu, X. W. Li, G. Q. Gong, Gang Xiao, A. Gupta, P. Lecoeur, J. Z. Sun, Y. Y. Wang, and V. P. Dravid, *Phys. Rev. B* 54, R8357 (1996);
    "Direct evidence for a half-metallic ferromagnet," J.-H. Park, E. Vescovo, H.-J. Kim, C. Kwon, R. Ramesh, and T. Venkatesan, *Nature* 392, 794 (1998)
11. "Band structure of the high temperature phase of Fe_3O_4," A. Yanase and K. Siratori, *J. Phys. Soc. Jpn*. 53, 312 (1984);
    "Electron states, magnetism, and the Verwey transition in magnetite," Z. Zhang and S. Satpathy, *Phys. Rev. B* 44, 13319 (1991)
12. "Observation of spin-polarized electron levels in ferrites," S. F. Alvarado, W. Eib, F. Meier, D. T. Pierce, K. Sattler, H. C. Siegmann, and J. P. Remeika, *Phys. Rev. Lett.* 34, 319 (1975);

"Final-state effects in the 3d photoelectron spectrum of Fe_3O_4 and comparison with Fe_xO," S. F. Alvarado, M. Erbudak, and P. Munz, *Phys. Rev. B* 14, 2740 (1976)

13. "Photoelectron spin polarization and ferromagnetism of crystalline and amorphous nickel," U. Bänninger, G. Busch, M. Campagna, and H. C. Siegmann, *Phys. Rev. Lett*. 25, 585 (1970)
14. "Spin polarized electrons and magnetism 2000," H. C. Siegmann, in: *Physics of Low Dimensional Systems*, edited by J. L. Morán-López (Kluwer Academic/Plenum Publishers, New York, Boston, Dordrecht, London, Moscow, 2001) pp. 1-14
15. "Spin polarization of photoelectrons and itinerant magnetism in iron," W. Eib and B. Reihl, *Phys. Rev. Lett*. 40, 1674 (1978);
"Spin-polarized surface states of Fe(100)," E. Vescovo, O. Rader, and C. Carbone, *Phys. Rev. B* 47, 13051 (1993);
"Magnetism of epitaxial bcc iron on Ag(001) observed by spin-polarized photoemission," M. Stampanoni, A. Vaterlaus, M. Aeschlimann, and F. Meier, *Phys. Rev. Lett.* 59, 2483 (1987)
16. "Spin-polarized photoelectrons from nickel single crystals," W. Eib and S. F. Alvarado, *Phys. Rev. Lett.* 37, 444 (1976)
17. "Spin-dependent tunneling into ferromagnetic nickel," P. M. Tedrow and R. Meservey, *Phys. Rev. Lett.* 26, 192 (1971)
18. "Spin polarized electron tunneling," R. Meservey and P. M. Tedrow, *Physics Reports* 238, 173 (1994)
19. "Spin-dependent tunnelling from transition-metal ferromagnets," J. A. Herz and K. Aoi, *Phys. Rev. B* 8, 3252 (1973)
20. "Modelling of spin-polarized tunnelling from 3d ferromagnets," E. Y. Tsymbal and D. G. Pettifor, *J. Phys. Cond. Matter.* 9, L4111 (1997)
21. "The role of electronic structure in magnetic tunneling," K. Wang, S. Zhang, P. M. Levy, L. Szunyough, and P. Wienberger, *J. Magn. Magn. Mater*. 189, L131 (1998)
22. "Tight-binding theory of tunneling giant magnetoresistance," J. Mathon, *Phys. Rev. B* 56, 11810 (1997)
23. "Simple explanation of tunneling spin-polarization of Fe, Co, Ni and its alloys," M. B. Stearns, *J. Magn. Magn. Mater*. 5, 167 (1977)
24. "Validity of the Jullière model of spin-dependent tunneling," J. M. MacLaren, X.-G. Zhang, and W. H. Buttler, *Phys. Rev. B* 56, 11827 (1997)
25. "Tunneling between ferromagnetic films," M. Jullière, *Phys. Lett*. 54, 225 (1975)
26. "Electron tunneling between ferromagnetic films," S. Maekawa and U. Gäfvert, *IEEE Trans. Magnetics* MAG-18(2), 707 (1982)
27. "Giant magnetic tunneling effect in Fe/Al_2O_3/Fe junction," T. Miyazaki and N. Tezuka, *J. Magn. Magn. Mat*. 139, L231 (1995)
28. "Large magnetoresistance at room temperature in ferromagnetic thin film tunnel junctions," J. S. Moodera, L. R. Kinder, T. M. Wong, and R. Meservey, *Phys. Rev. Lett*. 74, 3273 (1995)
29. "Exchange-biased magnetic tunnel junctions and application to nonvolatile magnetic random access memory," S. S. P. Parkin, K. P. Roche, M. G. Samant, P. M. Rice, R. B. Beyers, R. E. Scheuerlein, E. J. O'Sullivan, S. L. Brown, J. Bucchiagano, D. W. Abraham, Yu Lu, M. Rooks, P. L. Troulloud, R. A. Wanner, and W. J. Gallagher, *J. Appl. Phys*. 85, 5828 (1999)
30. "Review of recent results on spin polarized tunneling and magnetic switching by spin injection," A. Fert, A. Berthélemy, J. Ben Joussef, J.-P. Contour, V. Cros, J. M De Teresa, A. Hamzic, J. M. George, G. Faini, J. Grollier, H. Jaffrès, H. Le Gall, F. Montaigne, F. Pailloux, and F. Petroff, *Mat. Sci. Engin. B* 84, 1 (2001)
31. "Spin-dependent tunneling conductance of Fe|MgO|Fe sandwiches," W. H. Butler, X.-G. Zhang, T. C. Schulthess, J. M. MacLaren, *Phys. Rev. B* 63, 054416 (2001);
"Spin-dependent tunneling in epitaxial systems: Band dependence of conductance," J. M. MacLaren, W. H. Butler and X.-G. Zhang, *J. Appl. Phys*. 83, 6521 (1998)

32. “Spin polarized density of states and electron tunneling from Co/Al_2O_3 interface,” D. Nguen-Manh , E. Yu. Tsymbal, D. Pettifor, C. Arcangeli, R. Tank, O. K. Andersen, and A. Pasturel, *Mat. Res. Soc. Symp. Proc*. 492, 319 (1998)
33. “Reversed spin polarization at the Co(001)-HfO_2(001) interface,” P. K. de Boer, G. A. de Wijs, and R. A. de Groot, *Phys. Rev. Lett*. 58, 15422 (1998)
34. “Structural and electronic properties of $Co/Al_2O_3/Co$ magnetic tunnel junction from first principles,” I. I. Oleinik, E. Yu. Tsymbal, and D. G. Pettifor, *Phys. Rev. B* 62, 3952 (2000)
35. “Electronic analog of the electro-optic modulator,” S. Datta and B. Das, *Appl. Phys*. *Lett.* 56, 665 (1990)
36. “Spin-valve effects in a semiconductor field-effect transistor: A spintronic device,” S. Gardelis, C. G. Smith, C. H. W. Barnes, E. H. Linfield, and D. A. Ritchie, *Phys. Rev*. *B* 60, 7764 (1999)
37. See, for instance “Spin relaxation under optical orientation in semiconductors,” G. E. Pikus and A. N. Titkov, in *Optical Orientation*, edited by F. Meier and B. P. Zakharchenya, Vol. 8 of *Modern Problems in Condensed Matter Sciences*, Series edited by V. M. Agranovich and A. A. Maradudin) (North Holland Physics Publishing, Elsevier Science, Amsterdam, 1984), Chap. 3, pp. 73-132
38. “Resonant spin amplification in *n*-Type GaAs,” J. M. Kikkawa and D. D. Awschalom, *Phys. Rev. Lett*. 80, 4313 (1997); “Lateral drag of spin coherence in gallium arsenide,” J. M. Kikkawa and D. D. Awschalom, *Nature* 397, 139 (1999)
39. “Electrical spin injection in a ferromagnetic semiconductor heterostructure,” Y. Ohno, D. K. Young, B. Beschoten, F. Matsakura, H. Ohno, and D. D. Awshalom, *Nature* 402, 790 (1999)
40. “Injection and detection of a spin-polarized current in a light emitting diode,” R. Fiederling, M. Keim, G. Reuscher, W. Ossau, G. Schmidt, A. Waag, and L. W. Molenkamp, *Nature* 402, 787 (1999)
41. “Boundary resistance of the ferromagnetic-nonferromagnetic metal interface,” P. C. van Son, H. van Kempen, and P. Wyder, *Phys. Rev. Lett*. 58, 2271 (1987)
42. “Fundamental obstacle for electrical spin injection from a ferromagnetic metal into a diffusive semiconductor,” G. Schmidt, D. Ferrand, and L. W. Molenkamp, A. T. Filip, and B. J. van Wees, *Phys. Rev. B* 62, R4790 (2000)
43. “Complex impedance of a spin injecting junction,” E. I. Rashba, *Appl. Phys. Lett*. 80, 2329 (2002)
44. “Electron spin injection at a Schottky contact,” J. D. Albrecht and D. L. Smith, *Phys. Rev. B* 66, 113303-1 (2002)
45. “Theory of electrical spin injection: Tunnel contacts as a solution of the conductivity mismatch problem,” E. I. Rashba, *Phys. Rev. B* 62, R16267 (2000)
46. “Electrical spin injection into semiconductors,” D. L. Smith and R. N. Silver, *Phys. Rev. B* 64, 045323 (2001)
47. “Enhancement of spin injection from ferromagnetic metal into a two-dimensional electron gas using a tunnel barrier,” H. B. Heersche, Th. Schäpers, J. Nitta, and H. Takanayagi, *Phys. Rev. B* 64, 161307-1 (2001)
48. “Electric field dependent spin diffusion and spin injection into semiconductors,” Z. G. Yu and M. E. Flatté, *Phys. Rev. B* 66, 201202-1 (2002);

    “Spin diffusion and injection in semiconductor structures: Electric field effects,” Z. G. Yu and M. E. Flatté, *Phys. Rev. B* 66, 235302-1 (2002)
49. “Tunneling potential barrier dependence of electron spin polarization,” S. F. Alvarado, *Phys. Rev. Lett*. 75, 513 (1995)
50. “Spin-polarized scanning tunneling spectroscopy on Fe and Ni,” S. F. Alvarado, in *New Trends in Magnetism, Magnetic Material and Their Applications*, Proc. 2nd Latin-American Workshop, Guanajuato, Mexico, August 1993, edited by J. L. Morán-López and J. M. Sanchez (Plenum, New York, 1994) pp. 175-182

51. "Observation of spin-polarized-electron tunneling from a ferromagnet into GaAs," S. F. Alvarado and Ph. Renaud, *Phys. Rev. Lett*. 68(9), 1387 (1992)
52. "Spatially resolved spin-injection probability for gallium arsenide," V. P. LaBella, D. W. Dullock, Z. Ding, C. Emery, A. Venkatesan, W. F. Olivier, G.J . Salamo, P. M. Thibado, and M. Mortazavi, *Science* 292, 1518 (2001)
53. "Spin polarization of injected electrons," W. F. Egelhoff Jr., M. D. Stiles, D. P. Pappas, D. T. Pierce, J. M. Byers, M. B. Johnson, B. T. Jonker, S. F. Alvarado, J. F. Gregg, J. A. C. Bland, R. A. Buhrman, *Science* 296, 1195a (2002)
54. "Experimental search for the electrical spin injection in a semiconductor," A. T. Filip, B. H. Hoving, F. J. Jedema, and B. J. van Wees, *Phys. Rev. B* 62, 9996 (2000)
55. "Spin-valve effects in a semiconductor field-effect transistor: A spintronic device," S. Gardelis, C. G. Smith, C. H. W. Barnes, E. H. Linfield, and D. A. Ritchie, *Phys. Rev. B* 60, 7764 (1999)
56. "Spin injection into carbon nanotubes and possible applications in spin-resolved scannig tunnelling microscopy," D. Orgassa, G. J. Mankey, and H. Fijiwara, *Nanotechnology* 12, 281 (2001)
57. "Observation of spin injection at a ferromagnet-semiconductor interface," P. R. Hammar, B. R. Bennett, M. J. Yang, and Mark Johnson, *Phys. Rev. Lett*. 83, 203 (1999)
58. "Comment on 'Observation of spin injection at a ferromagnet-semiconductor interface'," B. J. van Wees, *Phys. Rev. Lett*. 84, 5023 (2000);
"Magnetoelectronic phenomena at a ferromagnet-semiconductor interface," F. G. Monzon, H. X. Tang, and M. L. Roukes, *Phys. Rev. Lett*. 84, 5022 (2000);
"Reply: Hammar et al.," P. R. Hammar, B. R. Bennett, M. J. Yang, and Mark Johnson, *Phys. Rev. Lett.* 84, 5024 (2000)
59. "Room-temperature spin injection from Fe into GaAs," H. J. Zhu, M. Ramsteiner, H. Kostial, M. Wassermeier, H.-P. Schönherr, and K. H. Ploog, *Phys. Rev. Lett*. 87, 01601 (2001)
60. "Efficient electrical spin injection from a magnetic metal/tunnel barrier contact into a semiconductor," A. T. Hanbicki, B. T. Jonker, G. Itskos, G. Kioseoglou, and A. Petrou, *Appl. Phys. Lett*. 80, 1240 (2002)
61. "Spin-polarized light emitting diode using metal/insulator/semiconductor structures," T. Manago and H. Akinaga, *Appl. Phys. Lett*. 81, 694 (2002)"
62. "Electrical spin injection in a ferromagnet/tunnel barrier/semiconductor heterostructure, V. F. Motsny, J. De Boeck, J. Das W. Van Roy, G. Borghs, E. Goovaerts, and V. I. Safarov, *Appl. Phys. Lett*. 81, 265 (2002)
63. The magnitude of P has been recalculated to take into account the effect of the refraction of the light when leaving the semiconductor, see Ref. [53].
64. "Magnetism at surfaces and interfaces," A. J. Freeman and C. L. Fu, in *Magnetic Properties of Low-Dimensional Systems*, *Springer Proceedings in Physics*, Vol. 14, edited by L. M. Falicov and J. L. Morán-López (Springer-Verlag, Berlin, Heidelberg, 1986), pp. 16-24
65. "Spin- and angle-resolved photoemission study of (110)Fe films grown on GaAs by molecular beam epitax," K. Schröder, G. A. Prinz, K.-H. Walker, and E. Kisker, *J. Appl. Phys.* 57, 3669 (1985)
66. "Surface states, surface magnetization, and electron-spin polarization: Ni(001)," C. S. Wang and A. J. Freeman, *Phys. Rev. B* 21, 4585 (1980), see also Ref. 49.
67. "Spin-polarized electronic structure of the Ni(001) surface and thin films," O. Jepsen, J. Madsen, and O. K. Andersen, *Phys. Rev. B* 26, 2790 (1982)
68. "Magnetism of the Ni(110) and Ni(100) surfaces: Local-spin-density-functional calculations using the thin-slab linearized augmented-plane-wave method," H. Krakauer and A. J. Freeman, *Phys. Rev B* 28, 610 (1983)
69. "Surface magnetism of the clean Ni(111) surface and of a Ni monolayer on Cu(111)," C. L. Fu and A. J. Freeman, *J. Physique (Paris)* 49, C8-1625 (1988)

70. "Observation of –100% spin-polarized photoelectrons from a transversely magnetized Ni(110) single crystal," E. Kisker, W. Gudat, E. Kuhlmann, R. Clauberg, and M. Campagna, *Phys. Rev. Lett*. 45, 2053 (1980)
71. "Crossover from negative to positive spin polarization in the photoyield from Ni(111) near threshold," E. Kisker, W. Gudat, M. Campagna, E. Kuhlmann, H. Hopster, and I. Moore, *Phys. Rev. Lett*. 43, 966 (1979)
72. "Spin polarization of electrons field emitted from single-crystal iron surfaces," M. Landolt and Y. Yafet, *Phys. Rev. Lett,* 40, 1401 (1978)
73. "Electron spin polarization in field emission from EuS-coated tungsten tips," N. Müller, W. Eckstein, W. Heiland, and W. Zinn, *Phys. Rev. Lett.* 29, 1651 (1972)
74. "Spin polarization of field-emitted electrons and magnetism at the (100) surface of Ni," M. Landolt and M. Campagna, *Phys. Rev. Lett.* 38, 663 (1977);
"Electron spin polarization in field emission," M. Landolt and M. Campagna, *Surf. Sci.* 70, 197 (1978)
75. "Band-structure effects in the field-induced tunneling of electrons from metals," J. W. Gadzuk, *Phys. Rev*. 182, 416 (1969)
76. "Band-structure calculation of the electron spin polarization in field emission from ferromagnetic nickel," B. A. Polizer and P. H. Cutler, *Phys. Rev. Lett*. 28, 1330 (1972)
77. "Theory of the spin polarization of field-emitted electrons from nickel," J.-N. Chazalviel and Y. Yafet, *Phys. Rev. B* 15, 1062 (1977)
78. *Field, Thermionic and Secondary Electron Emission Spectroscopy*, A. Modinos (Plenum Press, New York, 1984)
79. "Precession of the spin polarization of photoexcited conduction electrons in the band-bending region of GaAs (110)," H. Riechert, S. F. Alvarado, A. N. Titkov, and V. I. Safarov, *Phys. Rev. Lett*. 52, 2297 (1984)
80. "Splitting of the conduction bands of GaAs for $\vec{k}$ along [110]," N. E. Christensen and M. Cardona, *Solid State Commun*. 51, 491 (1984)
81. "Spontaneous spin polarization of photoelectrons from GaAs," S. F. Alvarado, H. Riechert, and N. E. Christensen, *Phys. Rev. Lett*. 55, 2716 (1985)
82. "Effect of bulk inversion asymmetry on [001], [110], and [111] GaAs/AlAs quantum wells," R. Eppenga and M. F. H. Schuurmans, *Phys. Rev. B* 37, 10923 (1988)
83. "Observation of spin precession in GaAs inversion layers using antilocalization," P. D. Dresselhaus, C. M. A. Papavassiliou, R. G. Wheeler and R. N. Sacks, *Phys. Rev. Lett*. 68, 106 (1992)
84. "Electron-metal-surface interaction potential with vacuum tunneling: Observation of the image force," G. Binnig, N. García, H. Rohrer, J. M. Soler, and F. Flores, *Phys. Rev. B* 30, 4816 (1984)
85. "Electric tunnel effect between disimilar electrodes separated by a thin insulating film," J. G. Simmons, *J. Appl. Phys.* 35, 2581 (1963)
86. *Introduction to Scanning Tunneling Microscopy*, C. J. Chen (Oxford University Press, 1993)
87. *Handbook of the Band Structure of Elemental Solids*, D. A. Papaconstantopoulos (Plenum, New York, 1986)
88. "Surface magnetism in iron, cobalt, and nickel," M. Aldén, M. Mirbt, H. L. Skriber, N. M. Rosengaard, and B. Johansson, *Phys. Rev. B* 46, 6303 (1992)
89. "The new generation of surface-specific, spin-sensitive spectroscopies," F. B. Dunning, C. Rau, and G. K. Walters, *Comments Solid State Physics* 12, 17 (1985)
90. "Theory of tunneling magnetoresistance," J. Mathon and A. Umerski, in: *Physics of Low Dimensional Systems*, edited by J.L. Morán-López (Kluwer Academic/Plenum Publishers, New York, Boston, Dordrecht, London, Moscow, 2001), pp. 363-372